Robotics and Autonomous Systems 174 (2024) 104642

Contents lists available at ScienceDirect

Robotics and Autonomous Systems

journal homepage: www.elsevier.com/locate/robot

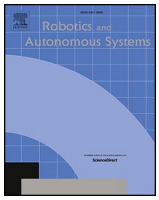

Optimizing the performance of a wheeled mobile robots for use in agriculture using a linear-quadratic regulator

Sairoel Amertet [a,*], Girma Gebresenbet [b], Hassan Mohammed Alwan [c]

[a] High School of Automation and Robotics, Peter the Great Saint Petersburg Polytechnic University, 195220 Saint Petersburg, Russia
[b] Department of Energy and Technology, Swedish University of Agricultural Sciences, P.O. Box 7032, 750 07 Uppsala, Sweden
[c] Department of mechanical Engineering, University of technology, Baghdad, Iraq

ARTICLE INFO

Keywords:
Wheeled mobile robot
Agriculture
Linear-quadratic regulator
Nonholonomic
Optimization

ABSTRACT

Use of wheeled mobile robot systems could be crucial in addressing some of the future issues facing agriculture. However, robot systems on wheels are currently unstable and require a control mechanism to increase stability, resulting in much research requirement to develop an appropriate controller algorithm for wheeled mobile robot systems. Proportional, integral, derivative (PID) controllers are currently widely used for this purpose, but the PID approach is frequently inappropriate due to disruptions or fluctuations in parameters. Other control approaches, such as linear-quadratic regulator (LQR) control, can be used to address some of the issues associated with PID controllers. In this study, a kinematic model of a four-wheel skid-steering mobile robot was developed to test the functionality of LQR control. Three scenarios (control cheap, non-zero state expensive; control expensive, non-zero state cheap; only non-zero state expensive) were examined using the characteristics of the wheeled mobile robot. Peak time, settling time, and rising time for cheap control based on these scenarios was found to be 0.1 s, 7.82 s, and 4.39 s, respectively.

1. Introduction

Research on wheeled mobile robot systems has expanded in the past 10 years, in order to deal with the complex dynamics, uncertainties, and rapidly shifting disturbances that such robotic systems encounter [1]. There are already numerous areas of application for wheeled mobile robots, in e.g., wireless-powered communication networks (WPCN), logistics, monitoring forest fires, military and civilian surveillance, and data collection and acquisition [2]. The range and quantity of applications will continue to increase in future with the emergence of improved features such as more compact size, maneuverability in confined spaces, and lower hardware mechanical complexity compared with other robotic systems [3].

However, wheeled mobile robots are more vulnerable to different kinds of disruptions and uncertainties when in operation, meaning that their control systems must be strong, reliable, and functional [4]. Various control systems have been suggested to regulate the dynamics of wheeled mobile robots. Some of these, such as linear-quadratic regulator (LQR), H-infinity, and proportional integral derivative (PID), are based on linear control theories. Other designs based on non-linear control theories, including model predictive control (MPC), feedback linearization, sliding-mode, and backstepping have also been developed [5–7]. Additionally, learning-based flight control theories and hybrid control, such fuzzy logic and neural networks, have been applied to regulate the dynamics of wheeled mobile robots. One of the best control approaches, which is predicated on minimizing a certain quadratic cost function, is LQR, which has been thoroughly studied for use in regulating the dynamics of wheeled mobile robots. The quadratic cost function of the LQR controller is composed of two weighting matrices, Q and R, where the Q matrix is linked to deviations in the trajectories of state variables and the R weighting matrix is related to actuator saturation and control effort [8–11].

The primary concern when using the LQR optimum controller for real-time applications is choosing appropriate values for the Q and R weighting matrices, which are trade-offs by nature and are typically changed via a trial-and-error method. For example, choosing large coefficient values for the R matrix penalizes the control effort more severely in order to optimize the cost function, resulting in an expensive control solution [12,13], while choosing very small values for the R matrix entails attempting to stabilize the system using an inexpensive control method. For the Q matrix, selecting large coefficient values means attempting to stabilize the system with the fewest feasible state

* Corresponding author.
E-mail address: sairoel@mtu.edu.et (S. Amertet).

https://doi.org/10.1016/j.robot.2024.104642
Received 25 October 2023; Received in revised form 14 January 2024; Accepted 25 January 2024
Available online 2 February 2024

changes, whereas selecting smaller values indicates less concern with state changes [14–17]. Designer experience and trial-and-error play a major role in selection, but the impacts of uncertainty and disturbance are not taken into account when modifying the weighted performance matrices Q and R through trial-and-error [18,19].

In addressing this area of concern, the durability and excellent performance of LQR controllers provide the capacity to minimize control effort while reducing deviations in the state trajectories of wheeled mobile robots [20–23]. The suitability of LQR control for a wheeled mobile robot for use in agriculture was analyzed in the present study. The remainder of this paper is arranged as follows: Section 2 describes the concept behind selection of the wheeled mobile robot model, Section 3 presents the mathematical models and control theory design applied in developing the model, and Section 4 describes and discusses the modeling outcomes for three scenarios (control cheap, non-zero state expensive; control expensive, non-zero state cheap; only non-zero state expensive). Some conclusions from the work are presented in Section 5.

2. Wheeled mobile robot model background and selection

At present, 6.4 % of global economic productivity is derived from agriculture and many countries worldwide have agriculture as their primary economic sector. In addition to providing billions of people with food, agriculture creates jobs for a sizable portion of the global population. Concerns about food security, the rapid rise in global population, and unexpected climate change have prompted the agriculture industry to look for new and creative ways to boost crop production. As a result of these efforts, wheeled mobile robots are gradually becoming more prevalent in the sector, as part of an ongoing technological revolution [24–30]. Table 1 shows the current issues and highlights recent progress in the field.

Types of wheeled mobile robots and their characteristics. The mobile robot in the agricultural fields was depicted in Fig. 1. The mobile robot is continuously monitoring the health of the crops during their growth.

Wheeled robots move over the ground by the action of motorized wheels. The wheel types currently available and their key characteristics are listed in Table 2.

Fig. 1. Wheeled mobile robot in action in the field [24].

Based on its superior characteristics, a four-wheeled robot design was selected for use in modeling in this study.

3. Development of a kinematic model of a four-wheeled mobile robot for agricultural applications

3.1. Case study and assumptions

Differential steering was assumed for the four-wheel undercarriage of the selected mobile robot, with each wheel operated separately through the use of a servomechanism (a recommended wheeled undercarriage design). Assumptions made when creating the kinematic model were that:

- Wheel deformations are small or constant
- Wheels roll without slipping

Table 1
recent work in the area.

Resources	Principal Findings of the Research
[31]	The goal of this work is to use a multi generic decision-making strategy to optimize the control system's algorithm for a collection of robotic assets. Many operator decision support techniques and control algorithms utilized by research teams to build heterogeneous robotic means to address agricultural monitoring tasks fall short of providing a complete solution. The method is based on model optimization, namely the idea of auctions inside the created system, which makes it possible to identify a robotic system that has the highest chance of completing the assigned task.
[32]	In this research, an adaptive control technique based on reinforcement learning is suggested to handle the input time delayed system and discrete-time (DT) nonlinear state tracking problem of the wheeled mobile robot (WMR). With the standard model of the WMR turned into an affine nonlinear DT system, a delay matrix function and appropriate Lyapunov-Krasovskii functionals are provided to overcome the issues caused by the state and input time delays, respectively. Moreover, adaptive laws are defined for the adaptive controller, the critic NN, and the action NN using the approximation of the radial basis function neural networks (NNs) to ensure the uniform ultimate boundedness of all signals in the WMR system and the tracking errors convergence to a small compact set to zero.
[33]	For such a goal, a discrete-time LQR (Linear Quadratic Regulator) predictive controller is created. The LQR predictive controller was successfully used to MIMO time-delay processes displaying huge, non-minimum phase modes, integrating, stable, and unstable modes in order to validate such an approach. The disturbances in the output were chosen at random.
[34]	Reinforcement learning is a model-free optimal control technique used in this work that interacts directly with the environment to optimize a control policy. Because of chattering in the goal state, common discrete-action approaches are not well suited for reaching goals that finish in regulation. Three approaches to solving this challenge by fusing traditional LQR control with reinforcement learning were compared by the authors. Specifically, they present an approach that incorporates LQR control into the action set, enabling generalization and preventing the need to fix the calculated control in the replay memory if it is derived from dynamics that have been learned. Moreover, incorporate LQR control into a strategy that uses continuous action. In both cases, they showed that adding LQR control can increase performance, although the effect is more substantial if it can be utilized to augment a discrete action set.
[35]	This study offers an application of Reinforcement Learning (RL) that makes use of a tracking controller based on the linear quadratic regulator (LQR) and enhanced by a tracking error component. In order to deal with the steady-state errors, Linear Quadratic Tracker with Integrator (LQTI) is constructed by adding an integration term of the tracking error in the state variable. For the tracking problem, an online learning approach based on Integral Reinforcement Learning (IRL) is used to identify the best control on the partially unknown continuous-time systems by adjusting the augmented state variable. This approach is based on the LQTI. Through numerical simulation on two applications, the performance of the method and the optimal control solution are confirmed.
This paper	Using wheeled mobile robot systems could prove essential to solving some of the challenges agriculture might encounter in the future. To assess how well LQR control worked, a kinematic model of a four-wheel skid-steering mobile robot was created. The features of the wheeled mobile robot were used to analyze three scenarios: only non-zero state expensive; control expensive, non-zero state cheap; and control cheap, non-zero state expensive.

Table 2
Types of wheels currently available for wheeled robots.

Parameter	Single-wheel [24–30]	Double-wheel [18–25]	Three-wheel [9–14]	Four-wheel [9–25]
Moving over a non-level surface	Extremely difficult to keep balanced due to single point of contact on ground	Difficult to stabilize	Stable	Most stable configuration
Center of gravity	Not properly located	Robot body is kept below the axle	Inside the triangle formed	Remains inside the rectangle formed
Number of inputs	Single	Double	Three	Four or more
Power usage	Small	More than with single wheels, less than with three wheels	More than with double wheels, less than with four wheels	High
Control	The most difficult	Better than with single wheels, worse than with three wheels	Better than with double wheels, worse than with three wheels	Best
Mathematical models	The simplest	Simple	Better than with four wheels	Complex
Route performance	The most difficult	Difficult	Better	Best

- Wheel roll is clean, so velocity at the middle of wheel is equal to peripheral speed
- Chassis velocity is low
- There is point contact between wheels and pad.

Such considerations are an inherent part of almost any task involving vehicle motion. An efficient and all-encompassing approach to vehicle motion is the so-called matrix kinematics method.

3.2. Skid-steering mobile robot (SSMR)

In the kinematic model, a skid-steering mobile robot (SSMR) was tested. It was assumed that this robot operated on a plane surface with an inertial orthonormal basis (X_g, Y_g, Z_g), as shown in Fig. 2.

A local coordinate, located by (X_l, Y_l, Z_l), was assigned to the robot at its center of mass (COM). From Fig. 2, the coordinates of COM in the inertial frame can be written as COM (X, Y, Z). Since only plane motion was considered in this study, the Z-coordinate of COM was constant ($Z =$ const). The robot was assumed to move on the plane surface with linear velocity expressed in the local frame as $V = |V_x\ V_y\ V_z|^T$ and to rotate with an angular velocity vector $\omega = [0\ 0\ \omega]^T$, where $q = |X\ Y\ \theta\ |^T$ is the state vector describing generalized coordinates of the robot (i.e., the COM position, X and Y, and the orientation θ of the local coordinate frame with respect to the inertial frame). Thus $\dot{q} = |\dot{X}\dot{Y}\dot{\theta}|^T$ denoted the vector of generalized velocities. The variables $\dot{X}$ *and* $\dot{Y}$ were related to coordinates as indicated in Fig. 3. Mathematically, the free-body kinematics equations were:

$$\begin{cases} X = \mathrm{X_{ICRx}}\sin\theta + \mathrm{X_{ICRy}}\cos\theta \\ Y = \mathrm{X_{ICRx}}\cos\theta + \mathrm{X_{ICRy}}\sin\theta \end{cases}$$

$$\begin{cases} \dfrac{dX}{dt} = \dot{X} = \dfrac{d}{d\theta}\left(\mathrm{X_{ICRx}}\sin\theta + \mathrm{X_{ICRy}}\cos\theta\right) \\ \dfrac{dY}{dt} = \dot{Y} = \dfrac{d}{d\theta}\left(\mathrm{X_{ICRx}}\cos\theta + \mathrm{X_{ICRy}}\sin\theta\right) \end{cases}$$

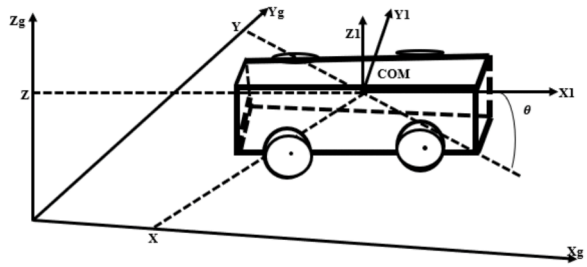

Fig. 2. Skid-steering mobile robot in the inertial frame (COM, center of mass) [28].

Using chain rules:

$$\begin{cases} \dfrac{dX}{dt} = \ddot{X} = \left(\mathrm{X_{ICRx}}\ddot{\theta}\cos\theta - \mathrm{X_{ICRy}}\dot{\theta}\sin\theta\right) \\ \dfrac{dY}{dt} = \ddot{Y} = \left(\mathrm{X_{ICRx}}\ddot{\theta}\sin\theta + X_{\mathrm{ICRy}}\dot{\theta}\cos\theta\right) \end{cases}$$

With:

$$\begin{cases} V_x = X_{ICRx}\dot{\theta} \\ V_y = X_{ICRy}\dot{\theta} \end{cases}$$

Where X_{ICRx}, local coordinate along x axis, X_{ICRy}, local coordinate along y axis.

Based on the [4], the system equation can then be written as:

$$\begin{bmatrix} \ddot{X}\ \ddot{Y} \end{bmatrix} = \begin{bmatrix} \cos\theta & -\sin\theta \\ \sin\theta & \cos\theta \end{bmatrix} \begin{bmatrix} V_x \\ V_y \end{bmatrix} \quad (1)$$

For planar motion, $\dot{\theta} = \omega$.

3.3. Relationship between wheel velocities and local velocities

For simplicity, the thickness of the wheel was neglected and the wheel was assumed to be in contact with the plane surface at point $\mathrm{P_i}$ in Fig. 3. In contrast to most wheeled vehicles, the lateral velocity of the SMRR (V_{iY}) is generally non-zero, where $i = 1, 2, 3, 4\ldots$. This property derives from the mechanical structure of the SSMR, which makes lateral skidding necessary if the vehicle changes its orientation. Therefore, the wheels are tangent to the path only if $\omega = 0$, at which the robot moves along a straight line. We considered only a simplified case of SSMR movement for which the longitudinal slip between the wheels and the surface can be neglected. Linear velocity was then related to angular velocity as $V_{iX} = r_i\omega_i$, where V_{iX} is the longitudinal component of the total velocity vector V_i of the i^{th} wheel expressed in the local frame and r_i *is* effective rolling radius of that wheel. To develop a kinematic model,

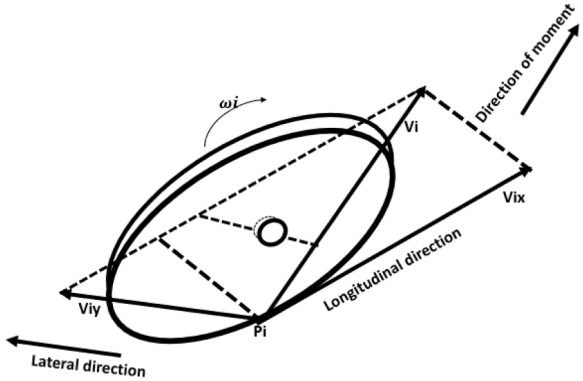

Fig. 3. Velocities at one wheel of the four-wheeled mobile robot (ω_i, angular velocity vector at point $\mathrm{P_i}$) [26].

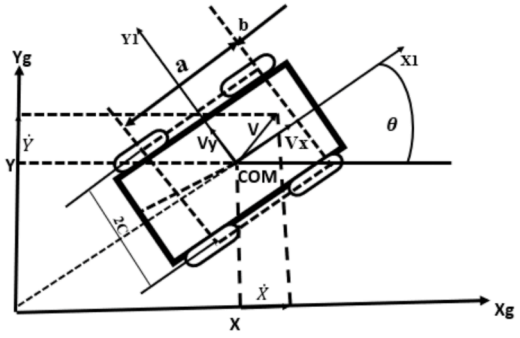

Fig. 4. Free body diagram of the four-wheeled mobile robot (COM, center of mass) [36].

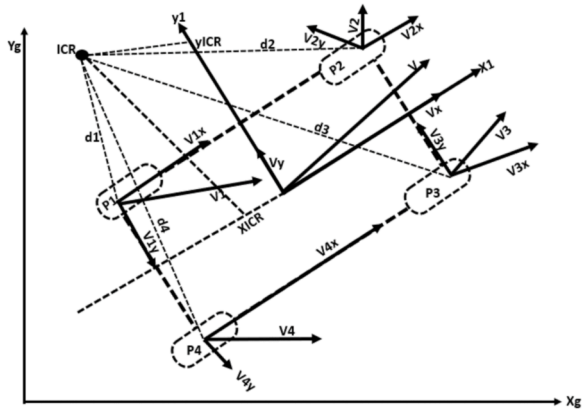

Fig. 5. Wheel velocities for the four-wheeled mobile robot [36].

it was necessary to take into consideration all four wheels together.

As shown in Fig. 4, the radius vectors then became $d_i = [d_{ix}\ d_{iy}]^T$, and $d_C = [d_{Cx}\ d_{Cy}]^T$, re-defined with respect to the local frame from the instantaneous center of rotation (ICR).

Based on the geometry in Fig. 5, the following expression was deduced: $\| \frac{V_i}{d_i} \| = \| \frac{V}{d_C} \| = |\omega|$. Accordingly [8–10], it is known from Euclidean norm equation that:

$$\frac{V_{ix}}{-d_{iy}} = \frac{V_x}{-d_{Cy}} = \frac{V_{iy}}{-d_{ix}} = \frac{V_y}{-d_{Cx}} = \omega. \tag{2}$$

From instantaneous center of rotation (ICR) in the local frame:

$$ICR = (X_{ICR},\ Y_{ICR}) = (-d_{Cx},\ d_{Cy}) \tag{3}$$

Then Eq. (2) becomes

$$\frac{V_x}{Y_{ICR}} = -\frac{V_y}{X_{ICR}} = \omega \tag{4}$$

From Fig. 5, it is clear that the coordinates of vectors d_i satisfy the following relationships:

$$\begin{cases} d_{1y} = d_{2y} = d_{Cy} + C \\ d_{3y} = d_{4y} = d_{Cy} - C \\ d_{1x} = d_{4x} = d_{Cx} - a \\ d_{2x} = d_{3x} = d_{Cx} + b \end{cases} \tag{5}$$

where a, b, and c are positive kinematic parameters for the robot depicted in Fig. 4.

On combining Eq. (2) and Eq. (5), the following relationships between wheel velocities were obtained:

$$\begin{cases} V_L = V_{1x} = V_{2x} \\ V_R = V_{3x} = V_{4x} \\ V_F = V_{2y} = V_{3y} \\ V_B = V_{1y} = V_{4y} \end{cases} \tag{6}$$

where V_L and V_R denote the longitudinal coordinates of the left and right wheel velocities, respectively, and V_F and V_B are the lateral coordinates of the velocities of the front and rear wheels, respectively. Then from Eq. (2) to Eq. (6), the relationship between the wheel velocities and the velocity of the robot is:

$$\begin{bmatrix} V_L \\ V_R \\ V_F \\ V_B \end{bmatrix} = \begin{bmatrix} 1 & -c \\ 1 & c \\ 0 & -x_{ICR} + b \\ 0 & -x_{ICR} - a \end{bmatrix} \begin{bmatrix} V_x \\ \omega \end{bmatrix} \tag{7}$$

Assuming that the effective radius is $r_i = r$ for each wheel, back substitution into Eq. (7) gives:

$$\begin{bmatrix} \omega_L \\ \omega_R \end{bmatrix} = \frac{1}{r} \begin{bmatrix} V_L \\ V_R \end{bmatrix} \tag{8}$$

where ω_L are ω_R is the angular velocity of the left and right wheels, respectively.

Combining eqs. (7) and (8), the following approximate relationship between the angular wheel velocities and the velocities of the robot was developed (which was the rod profile for the robotics):

$$\beta = \begin{bmatrix} V_x \\ \omega \end{bmatrix} = r \begin{bmatrix} \frac{\omega_L + \omega_R}{2} \\ \frac{-\omega_L + \omega_R}{2c} \end{bmatrix} \tag{9}$$

where β is a new control input introduced at the kinematic level.

From Eq. (9) it is clear that, theoretically, the pair of velocities ω_L and ω_R can be treated as a control kinematic input signal, as can velocities V_x and ω. However, longitudinal slip has a major role in the precision of the relationship in Eq. (9), which can only hold true if longitudinal slip is not prominent. To guarantee high validity in determination of the angular velocity of the robot with regard to the angular velocities of the wheels, the parameters R and C in Eq. (9) can also be determined experimentally. If a velocity constraint is introduced in the system, then:

$$V_y + x_{ICR}\dot{\theta} = 0 \tag{10}$$

Eq. (10) is not integrable and is consequently a nonholonomic constraint. It can therefore be rewritten in the form $[-\sin\theta\ \cos\theta\ x_{ICR}]$ $[\dot{x}\dot{y}\dot{\theta}] = A(q)\dot{q} = 0$, where Eq. (1) is used. Since the generalized velocity $\dot{q}$ is always in the null space of A, then:

$$\begin{cases} \dot{q} = S(q)^* \beta S^T(q) A^T(q) = 0 \\ S(q) = \begin{bmatrix} \cos\theta & x_{ICR}\sin\theta \\ \sin\theta & -x_{ICR}\cos\theta \\ 0 & 1 \end{bmatrix} \end{cases} \tag{11}$$

It should be noted that dim $(\beta) = 2 <$ dim $(q) = 3$. Eq. (7) describes the kinematics of the robot, which is underactuated. This is also a nonholonomic system, because of the constraint described by Eq. (10). It is interesting to note that the kinematic model of the SSMR analyzed was quite similar to the kinematics of a two-wheeled mobile robot. From Eqs. (4) and (7), it can be seen that control of the V_y and V_{yi} velocity coordinates is not possible without knowledge of the xl-axis projection of the ICR. Therefore, considering the linear velocity V_x and the angular velocity ω as control signals seems to have an advantage over the previous parameters proposed. Instead of ω, velocity V_y was used in this study.

3.4. Validation of control of the linear wheeled mobile robot model

Control models must be holonomic systems with controllability or influence, i.e., control or influence is impossible if the model is non-holonomic. The concept of 'controllable' was created here in order to test this. Controllability can be roughly defined as the capacity to manipulate a system throughout its configuration space using specific permitted manipulations. A deterministic system is fully described at any given time by its state, which is the set of values of all its state variables (those variables defined by dynamic equations). Specifically, if the current and future values of the control variables (those whose values may be chosen) are known, and if the states of the system are known, then no information about the system's past is required to aid in future prediction. The system that the state space representation simulates is controllable if there is an input sequence that can move the system state from x_0 to x_f in a finite amount of time for any initial state, x_0, and any final state, x_f :

$$\begin{cases} \dot{x} = Ax(t) + Bu(t) \\ y = Cx(t) + Du(t) \end{cases} \tag{12}$$

There exists a control u from state x_0 at time t_0 to state x_1 at time $t_1 > t_0$ if and only if $x_1 - \varnothing(t_0, t_1)x_0$. The state-transition matrix $\varnothing$ is also smooth. We introduced the *nxm* matrix-valued function $M_0(t) = \varnothing(t_0, t)B(t)$ to give:

$$M_k(t) = \frac{d^k M_0}{dt^k}(t),\ k \geq 0 \tag{13}$$

We then examined the matrix of matrix-valued functions created by enumerating each column of the $M_i,\ i = 0, 1, \ldots k$:

$$M^{(k)}(t) = [M_0(t), \ldots . M_k(t)] \tag{14}$$

If there exists a $\widehat{t} = \in [t_0, t]$ and a non-negative integer k such that $rank\ M^{(k)}(\widehat{t}) = n$, then given the state $x(0)$ at an initial time, arbitrarily denoted $k = 0$, the state equation gives $x(1) = Ax(0) + Bu(0)$, and $x(2) = Ax(1) + Bu(1) = A^2x(0) + ABu(0) + Bu(1)$, and so on with repeated back-substitutions of the state variable, eventually yielding:

$$x(n) = Bu(n-1)ABu(n-2) + A^{n-1}Bu(0) + A^n x(0).$$

Equivalently:

$$x(n) - A^n x(0) = \left[B\ AB \ldots . A^{n-1}B\right]\left[u^T(n-1)\ u^T(n-2) \ldots . . u^T(0)\right]^T \tag{15}$$

At angle $= 30^o$ and $x_{ICR} = 0.6$ cm, the state matrix becomes:

$$A = \begin{bmatrix} 0.5 & 0 & 0 \\ 0.5 & -0.3 & 0 \\ 0 & 0 & 1 \end{bmatrix}$$

$$B = \begin{bmatrix} 0.5 \\ 0 \\ 0 \end{bmatrix}$$

$$C = [1\ 0\ 0]$$

$$D = 0$$

$$C_{controllable} = \begin{bmatrix} 0.5 & 0.25 & 0.125 \\ 0 & 0.25 & 0.05 \\ 0 & 0 & 0 \end{bmatrix}$$

$$Uncontrollable = Length(A) - Rank(controllable)$$

$$Length(A) = 3$$

$$Rank(controllable) = 2$$

$$Uncontrollable = 3 - 2 = 1$$

The observable of a wheeled mobile robot system is a measure of how well the system's internal states can be deduced from information about its exterior outputs.

The observable matrix is:

$$Observable = \begin{bmatrix} 1 & 0 & 0 \\ 0.5 & 0 & 0 \\ 0.25 & 0 & 0 \end{bmatrix}$$

$$Unonservable = length(A) - rank(observable)$$

$$Unonservable = 3 - 2 = 1$$

As a result, mobile robots on wheels are uncontrollable and invisible. This indicates that the system is nonholonomic, validating the mathematical models established.

Consequently, the projected state space matrix becomes:

$$S(q) = \begin{bmatrix} \cos & \theta\, x_{ICR}\sin\theta \\ \sin\theta & -x_{ICR}\cos\theta \end{bmatrix} \tag{16}$$

And the input matrix is Eq. (9).

3.5. Control system for the wheeled mobile robot model

Framework for LQR gain design

The goal of optimal control theory is to minimize costs while regulating a dynamic system. The Q problem is the situation in which a quadratic function describes the cost and a set of linear differential equations describe the dynamics of the system. A mathematical technique is used to find the settings of a (regulatory) controller that governs wheeled mobile robots. The algorithm minimizes a cost function with required weighting factors. An event or the values of one or more variables are mapped onto a real number that intuitively represents some "cost" related to the event via a cost function. A prevalent description of the cost function is the total of the important measurements' deviations from the desired values, such as the wheeled mobile robot's state. Thus, the controller settings that minimize unwanted deviations are found by the algorithm. The cost function may also take into account the size of the control action itself [31].

To solve for the optimal control and examine the properties of the closed loop system. Consider the following linear-time-invariant wheeled mobile robot model at angle $= 30^o$ and $x_{ICR} = 0.6$ cm, the state matrix becomes: $\dot{x} = Ax + Bu$,

$$A = \begin{bmatrix} 0.86 & 0.3 \\ 0.5 & -0.52 \end{bmatrix}$$

$$B = \begin{bmatrix} 0.5 \\ 0 \end{bmatrix}$$

With the performance index

$$\begin{cases} J = \int_0^{+\infty} \left(x_1^2 + ru^2\right)dt \\ Q = \begin{bmatrix} 1 & 0 \\ 0 & 0 \end{bmatrix},\ R = r \end{cases} \tag{17}$$

The eigenvalues of the open loop system are $0.5,\ -0.3$, and 1. In the performance index the state penalty matrix Q penalized the first state of the system. The controller penalty r left as a parameter, so it could be seen how small and large values of r changes the closed loop dynamics. It is always important to check if the design problem is well-posed. Conditions on the plant and on the performance index for well-posed problem require to check if the unstable modes of the system are controllable and if the unstable modes are observable through the state penalty matrix. To verify if $(A,\ B)$ is stabilizable and $\left(A,\ Q^{\frac{1}{2}}\right)$ is detectable. Now computing the controllable matrix:

$$\begin{cases} P_C = [B \quad AB] \\ \begin{bmatrix} 0.5 & 0.43 \\ 0 & 0.25 \end{bmatrix} \\ Rank = 2 \end{cases}$$

Since the matrix has full rank, the system is controllable. So, any unstable modes are controllable. Next, it can factor the state penalty matrix into square roots

$$Q = \left(Q^{\frac{1}{2}}\right)^T Q^{\frac{1}{2}} = \begin{bmatrix} 1 & 0 \\ 0 & 0 \end{bmatrix} * \begin{bmatrix} 1 & 0 \\ 0 & 0 \end{bmatrix} = \begin{bmatrix} 1 & 0 \\ 0 & 0 \end{bmatrix}$$

And then check the observability using the square root of Q:

$$\begin{bmatrix} Q^{\frac{1}{2}} \\ Q^{\frac{1}{2}}A \end{bmatrix} = \begin{bmatrix} 1 & 0 \\ 0 & 0 \\ 0.86 & 0.3 \\ 0 & 0 \end{bmatrix}, \; Rank = 2$$

Since this matrix has full rank, all modes of the system are observable through the penalty matrix. Now it can solve the algebraic riccati equation (ARE) [31]

$$PA + A^T P - PBR^{-1}B^T + Q = 0 \tag{18}$$

For P, using $A, B, Q,$ and $R = r$. Let $P = \begin{bmatrix} P_1 & P_2 \\ P_2 & P_3 \end{bmatrix}$. Then the ARE is

$$\begin{bmatrix} P_1 & P_2 \\ P_2 & P_3 \end{bmatrix}\begin{bmatrix} 0 & 1 \\ 0 & -1 \end{bmatrix} + \begin{bmatrix} 0 & 0 \\ 1 & -1 \end{bmatrix}\begin{bmatrix} P_1 & P_2 \\ P_2 & P_3 \end{bmatrix} - \begin{bmatrix} P_1 & P_2 \\ P_2 & P_3 \end{bmatrix}\begin{bmatrix} 0 \\ 1 \end{bmatrix}\frac{1}{r}[0 \; 1]*\begin{bmatrix} P_1 & P_2 \\ P_2 & P_3 \end{bmatrix} + \begin{bmatrix} 1 & 0 \\ 0 & 0 \end{bmatrix} = 0 \tag{19}$$

Since the riccati matrix P must be real symmetric and positive define, from Eq. (19), it can derive three equations for P_1, P_2, and P_3. These are

$$-\frac{P_2^2}{r} + 1 = 0 \tag{20}$$

$$1 - P_2 - \frac{P_2^2}{r} = 0 \tag{21}$$

$$2(P_2 - P_3) - \frac{P_3^2}{r} = 0 \tag{22}$$

The first equation gives $P_2 = \sqrt{r}$, both positive and negative values of m must be checked to see which is the solutions. Using $P_2 = \sqrt{r}$, P_1, *and* P_3 are

$$P_3 = r\left(\sqrt{1 + \frac{2}{\sqrt{r}}} - 1\right) \tag{23}$$

$$P_1 = \sqrt{r\sqrt{1 + \frac{2}{\sqrt{r}}}} \tag{24}$$

The constant state feedback gain matrix is

$$K = R^{-1}B^T P = \left[\frac{2}{\sqrt{r}} \quad \sqrt{1 + \frac{2}{\sqrt{r}}}\right] \tag{25}$$

Then the closed loop state dynamics characteristics equations become

$$\varnothing_{cl}(s) = s^2 + s\sqrt{1 + \frac{2}{\sqrt{r}}} + \frac{1}{\sqrt{r}} \tag{26}$$

the values of the optimal feedback gains are proportional to the relative magnitude of the Q and R. for a fixed R value, large values of Q heavily penalize the state relative to the control, the resulting optimal feedback gains grow large, and the closed-loop system response gets fast. On the other hand, small values of Q penalize the control more than the state, resulting in smaller control efforts. This keeps the gains small, producing a slower response. Common issues in the realm of control include how the output system can follow a reference in addition to the stabilization system. If the output is to follow reference *r*, then an integrator should be added and the error state (γ) should be defined as the integrator output, with γ representing the difference between the input and output of the wheeled mobile robot system:

$$\begin{cases} \dot{x} = Ax + Bu \\ y = Cx \\ u = -Kx + k_I\gamma \\ \dot{\gamma} = r - y = r - Cx \end{cases} \tag{27}$$

where x is a state vector, u is control signal, y is output, r is reference (step function, scalar), and γ is integrator output.

The kinematic system in Eq. (17) can be written as:

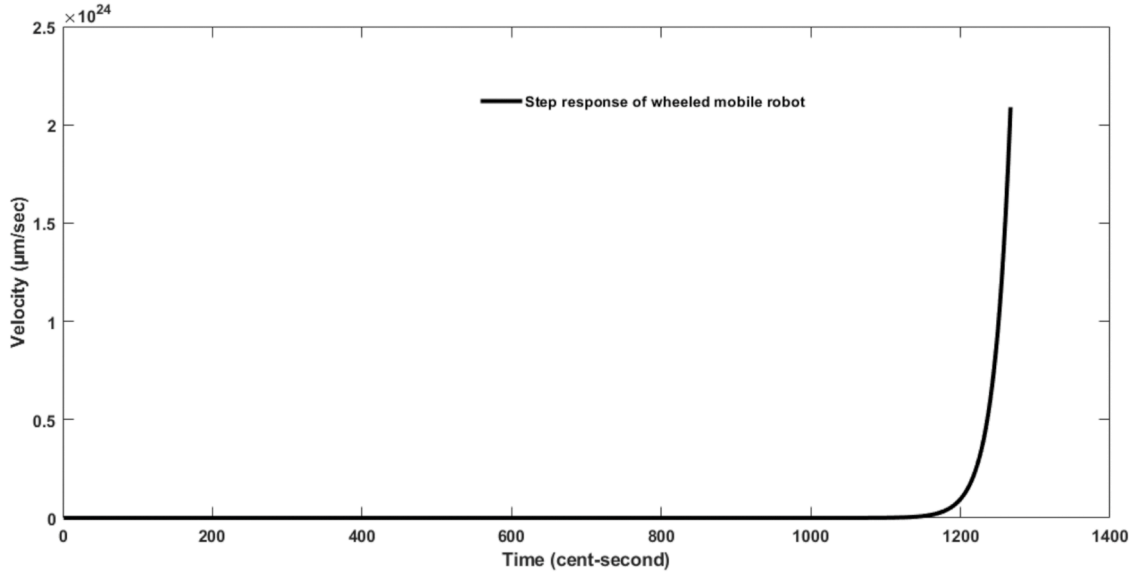

Fig. 6. Step response of the wheeled robot without a control mechanism.

$$\begin{cases} \begin{bmatrix} \dot{x} \\ \dot{y} \end{bmatrix} = \begin{bmatrix} A & 0 \\ -C & 0 \end{bmatrix} \begin{bmatrix} x \\ \gamma \end{bmatrix} + \begin{bmatrix} B \\ 0 \end{bmatrix} u + \begin{bmatrix} 0 \\ I \end{bmatrix} r \\ \begin{bmatrix} \dot{x}(\infty) \\ \dot{y}(\infty) \end{bmatrix} = \begin{bmatrix} A & 0 \\ -C & 0 \end{bmatrix} \begin{bmatrix} x(\infty) \\ \gamma(\infty) \end{bmatrix} + \begin{bmatrix} B \\ 0 \end{bmatrix} u(\infty) + \begin{bmatrix} 0 \\ I \end{bmatrix} r(\infty) \end{cases} \tag{28}$$

Tracking must be designed to make system stabilize. If $x(\infty), \gamma(\infty)$ *and* $u(\infty)$ approach constant values, then $\dot{\gamma} = 0$, *so* $y(\infty) = r$. In steady state, Eq. (18), because r(t) is signal step, then $r(\infty) = r(t) = r$ is constant value. For $t > 0$ subtracting Eq. (18) gives:

$$\begin{bmatrix} \dot{x}(t) - \dot{x}(\infty) \\ \dot{y}(t) - \dot{y}(\infty) \end{bmatrix} = \begin{bmatrix} A & 0 \\ -C & 0 \end{bmatrix} \begin{bmatrix} x(t) - x(\infty) \\ \gamma(t) - \gamma(\infty) \end{bmatrix} + \begin{bmatrix} B \\ 0 \end{bmatrix} [u(t) - u(\infty)] \tag{29}$$

This implies that:

$$\begin{cases} x(t) - x(\infty) = x_e(t) \\ \gamma(t) - \gamma(\infty) = \gamma_e(t) \\ u(t) - u(\infty) = u_e(t) \\ \begin{bmatrix} \dot{x}_e(t) \\ \dot{\gamma}_e(t) \end{bmatrix} = \begin{bmatrix} A & 0 \\ -C & 0 \end{bmatrix} \begin{bmatrix} x_e(t) \\ \gamma_e(t) \end{bmatrix} + \begin{bmatrix} B \\ 0 \end{bmatrix} [u_e(t)] \\ u_e(t) = -Kx_e(t) + K_I\gamma_e(t) \end{cases} \tag{30}$$

Vector error size $(n + 1)$ can be defined as: $e(t) = \begin{bmatrix} x_e(t) \\ \gamma_e(t) \end{bmatrix}$

Then Eq. (20) becomes: $\dot{e} = \hat{A}e + \hat{B}ue$, *with*: $\hat{A} = \begin{bmatrix} A & 0 \\ -C & 0 \end{bmatrix}$, $\hat{B} = \begin{bmatrix} B \\ 0 \end{bmatrix}$, into: $u_e = \hat{K}e$, $\hat{K} = [K\ K_I]$, into: $\dot{e} = (\hat{A} - \hat{B} * \hat{K})e$. The value of $\hat{K}$ is found with the LQR method and the cost function in LQR is defined by solving the optimization problem to (J)min:

$$J = \int_0^{+\infty} \left(x^T Q x + u^T R u\right) dt$$

Subject to:

$$\begin{cases} x = Ax + Bu \\ u(t) = -Kx(t) \end{cases} \tag{31}$$

where $K = R^{-1}B^T S$, which are full-state feedback controllers and where S is the solution to Riccati's algebraic equation (nxn) and $A^T S + SA - SBR^{-1}B^T S + Q = 0$.

3.6. Linear characteristics analyzed for the different scenarios

Settling time (T_S), i.e., the time required for the output to stabilize within a given tolerance band, is described mathematically as:

$$T_s = \begin{cases} \dfrac{4}{\sigma\omega_n}, & 0 < \sigma < 1 \\ \infty & \sigma = 0 \\ \dfrac{6}{\omega_n} & \sigma > 1 \end{cases} \tag{32}$$

where σ is damped ratio.

Rise time (T_r) describes the time taken for the solution to increase from 0 % to 100 % of its ultimate value in underdamped systems, or from 10 % to 90 % of its final value in over-damped systems. Mathematically:

$$Tr = \frac{\pi - \theta}{\omega_d} \tag{33}$$

Peak time (T_p) is the time required for the response to reach the peak value for the first time. Mathematically:

$$Tp = \frac{\pi}{\omega_d} \tag{34}$$

Peak overshoot, or maximum overshoot (M_p), is defined as the deviation of the response at peak time from the final value of response. It is expressed as:

$$Mp = \left(e^{-\left(\frac{\sigma\pi}{\sqrt{1-\sigma^2}}\right)}\right) * 100 \tag{35}$$

At steady state time (T_{ss}), the rate of input is equal to the rate of elimination

3.7. Theoretical analysis of the proposed results

Let assumed the difference between y and steady state. If that goes to zero, then the state space is stable. If that blows up, if y goes further away from the steady state, it's unstable. So $\frac{dy}{dt}$ is f of y. the capital $\frac{dY}{dt}$ well, that's actually 0. Capital Y is that constant steady state, and at the same time, f of y is 0. So, we have just put a 0 on the left side, and 0 on

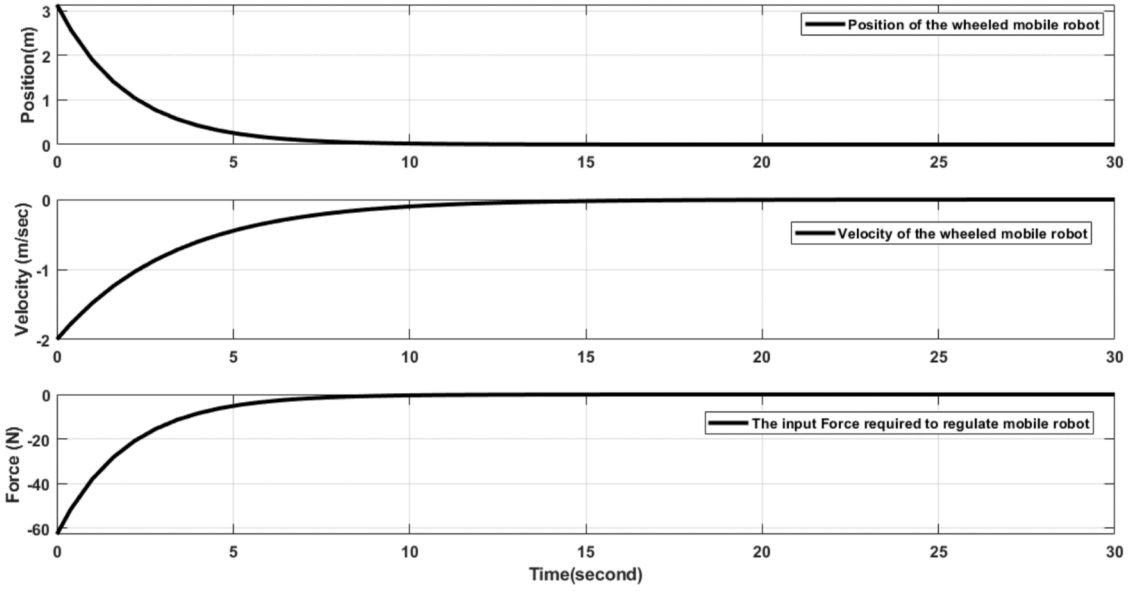

Fig. 7. Position, velocity, and force states in cheap control of the wheeled mobile robot.

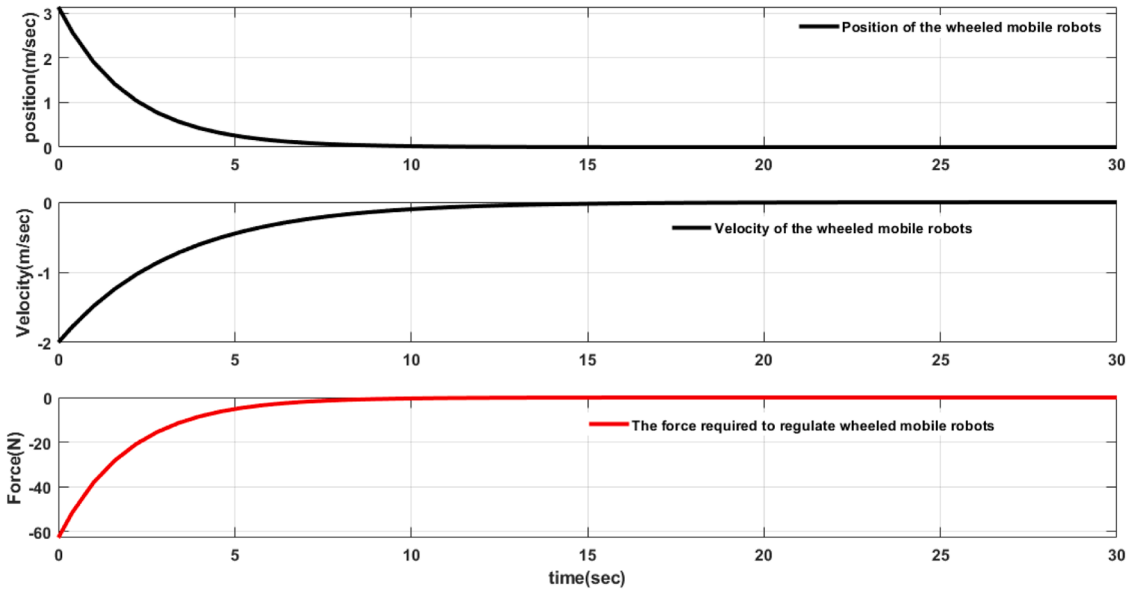

Fig. 8. Position, velocity, and force states in expensive control of the wheeled mobile robot.

the right side, remembering capital Y solves the equation with no movement at all.

Mathematically,

$$\frac{dy}{dt}(y-Y)=f(y)-f(Y) \tag{36}$$

To ensure the Eq. (36), let look at the derivative of state space from Eq. (16) before, and after applied the LQR algorithm.

Before applied LQR, let assumed that, $y = x$, and $\frac{dy}{dt} = \frac{dx}{dt} = \dot{x}$

$$\begin{cases} \frac{dy}{dt} = \dot{x}_1 = \mathrm{x}_1{}^*\cos\theta + x_2{}^* x_{ICR}\sin\theta \\ \frac{dy}{dt} = \dot{x}_2 = \mathrm{x}_1{}^*\sin\theta - x_2{}^*\cos\theta \end{cases} \tag{37}$$

At $\theta = 0$, between $\theta = 90$

The state space is positive this clamed that the state space without the control is unstable. However, the state after applied the control algorithms goes to 0, which implies that $y = Y$, if $\frac{dy}{dt} < 0$ then the state space is stable.

4. Simulation results and discussion

4.1. Results for the wheeled robot model without control

The velocity/time plot indicated that the wheeled model without control was totally unstable (Fig. 6). A mathematical representation of a physical system consisting of a set of road profiles (input), outputs, and variables connected by first-order differential equations or difference equations without the use of second derivatives (state-space representation) was developed for the system. These variables fluctuated over time in a way that depended on their current value and the values of other externally imposed variables. For example, the values of the output variables were influenced by the values of the state variables. Over the first 20 s, the wheeled robot remained stable with no disturbance, but after 21 s the system started to become unstable (slow disturbance) (Fig. 6). For the wheeled mobile robot system, no settling time, rise time, peak time, or steady state time could be obtained. This was due to the low impact that the wheeled robot sustained and the irregular movement on a rough surface, which caused instability in the system as a whole. After the model was updated with an appropriate controller system, the system became stable. This model was a linear state space representation, because the set of first-order differential equations was linear in the state and road profiles (input) variables. Linear quadratic regulation (LQR) was the selected control type.

A LQR controller for the wheeled mobile robot was built up mathematically by minimizing the cost function with selected weighting factors. Total departure of significant measures from ideal values, such as height, road profiles, or ground surface, is sometimes used to characterize the cost function. The LQR program then determines the controller settings that minimize unwanted deviations. The size of the control action itself may also be considered by the cost function.

4.2. Results for the wheeled robot model with LQR controller

Bryson's method was used to modify the Q and R weighting matrices, in an effort to address the shortcomings of the trial-and-error approach. Q and R were computed with this method by calculating the reciprocal of squares of the maximum permissible values of the state and input control variables. As Fig. 7 shows, a non-zero state was expensive and control was inexpensive. Because of this, the position of the wheeled mobile robots dropped for 5 s, before stabilizing at a less expensive position (Fig. 7). Concurrently, the velocity of the wheeled mobile robot system increased for 10 s before stabilizing throughout, because the velocity's state was far more expensive than the position of the mobile robot on its wheels. The force needed to stabilize the entire system was not very expensive for all non-zero states. This low cost and negative increase indicated that more control was used for controlling non-zero situations. By choosing modest coefficients, attempts were made to stabilize the system using a relatively cheap control method.

When non-zero states were inexpensive, control was costly (Fig. 8). Because of this, the position of the wheeled mobile robot system dropped until 8 s later, at which point it stabilized. The state of position was less expensive in this way. Concurrently, velocity of the wheeled mobile robot system velocity increased for 10 s, before stabilizing throughout, because the velocity's state was far more expensive than the position of the mobile robot on wheels. The force needed to stabilize the entire system was quite costly for all non-zero states, with the negative increase indicating that more control was needed to manage the non-zero states (Fig. 8). Selection of values for the Q and R weighting matrices, which involves trade-offs and is typically changed by trial-and-error, is the primary determinant of the LQR optimum controller for wheeled mobile robotics systems in real-time applications. On choosing large coefficients for the R matrix, control is sacrificed in order to optimize the cost

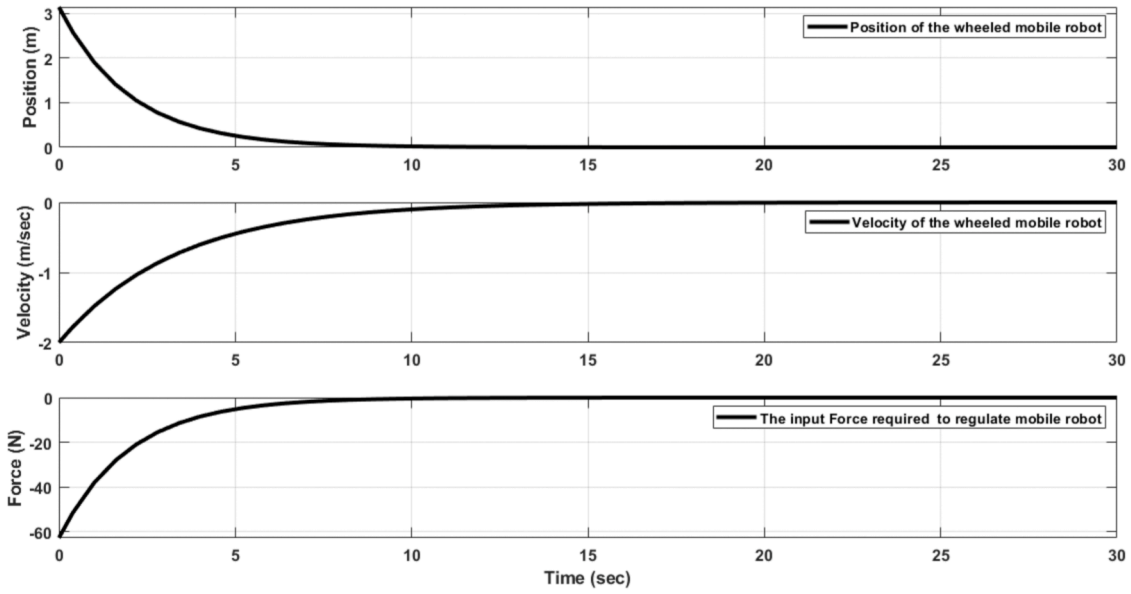

Fig. 9. Position, velocity, and force states of the wheeled mobile robot when ignoring the position.

function (expensive control).

Selecting large coefficients for the Q matrix stabilized the system with the fewest feasible state changes, whereas selecting lower values for Q ignored state changes (Fig. 9). In both these cases, experience and trial-and-error play a major role and the impacts of uncertainty and disturbance are not taken into account. A primary weakness of Bryson's rule is that it ignores disruptions and uncertainty and instead primarily relies on the designer's experience. Using Bryson's method as a starting point for choosing Q and R values, followed by applying the trial-and-error method to acquire the desired attributes of the closed-loop system, caused the response in expensive control to become comparable to that of the cheap solution (Fig. 9).

Peak time, settling time, rising time, and steady state time for the three different scenarios analyzed are shown in Table 3.

Table 3
Linear characteristics of the wheeled mobile robot in the different control scenarios analyzed.

Scenario	R (input penalization matrix)	Q (state penalization matrix)	K (Gain values)	Peak time (T_P, s)	Settling time (T_s, s)	Rise time (T_r, s)	Steady state time (T_{ss}, s)
Control cheap, non-zero state expensive	[0.01]	$\begin{bmatrix} 1 & 0 \\ 0 & 1 \end{bmatrix}$	[24.14 0]	0.0707	5.53	3.11	0.0707
Control expensive, non-zero state cheap	[1000]	$\begin{bmatrix} 1 & 0 \\ 0 & 1 \end{bmatrix}$	[20 0]	0.1	7.82	4.39	0.1
Only non-zero velocity expensive	[1]	$\begin{bmatrix} 0.001 & 0 \\ 0 & 10 \end{bmatrix}$	[20 0]	0.1	7.82	4.39	0.1

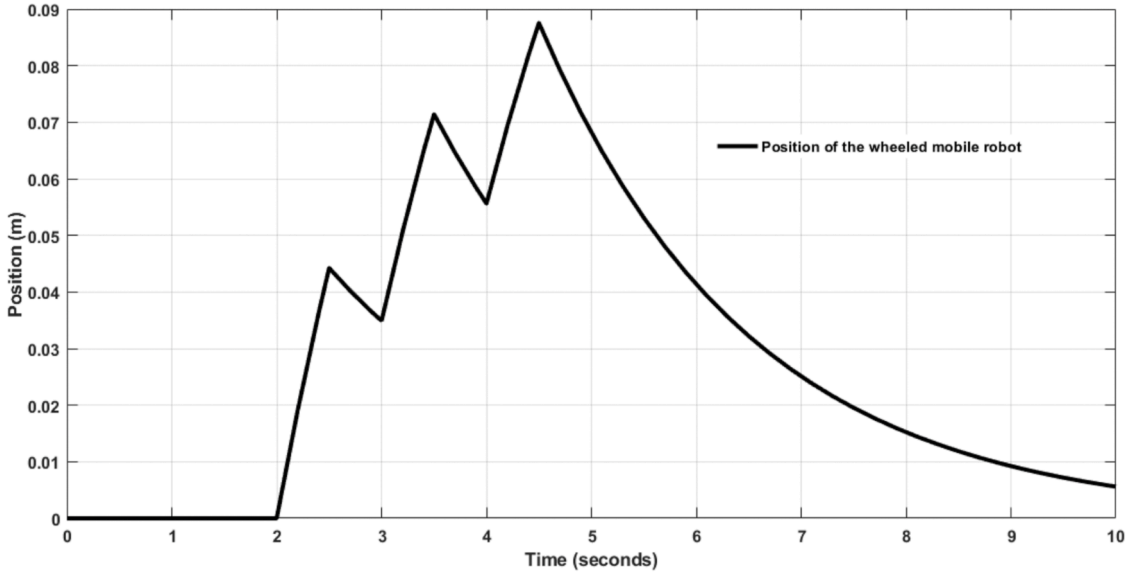

Fig. 10. Positions of wheeled mobile robot with the with linear-quadratic regulator (LQR) control system.

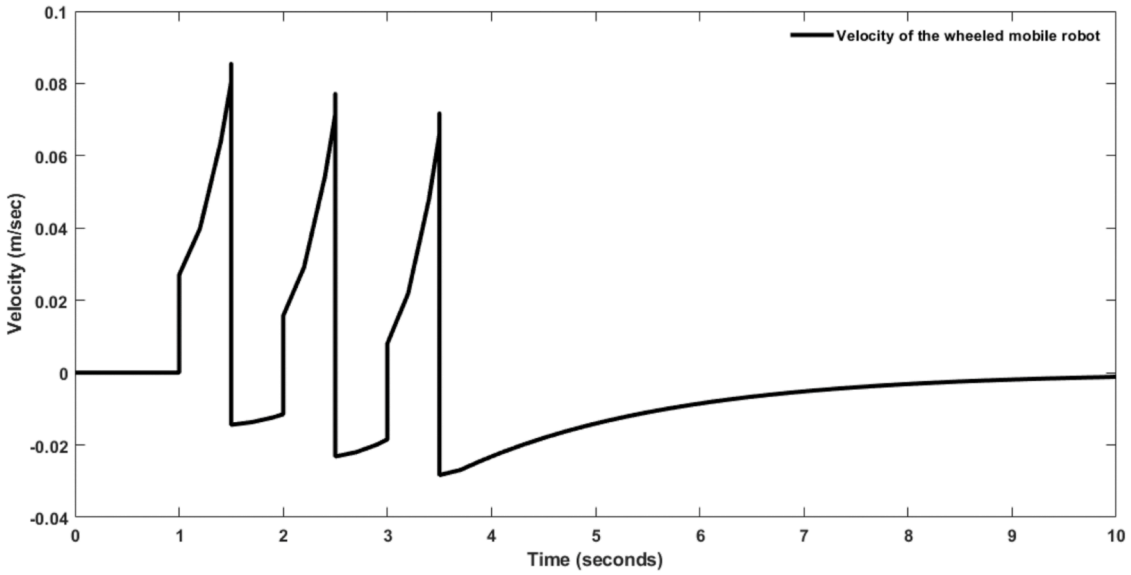

Fig. 11. Velocity response of the wheeled mobile robot with the linear-quadratic regulator (LQR) control system.

The vertical axis in Fig. 10 shows the position (in m) of the wheeled mobile robot, while the horizontal axis shows the time horizon. Three pumped road profiles were used as inputs after the proper feedback gains were optimally regulated to allow for closed-loop stable and high-performance system design. The system had to be stable for the robotic arm to stand on it when the correct control gains were applied.

Fig. 11 shows the response speed of the wheeled mobile robot. Three road profiles with bumps were applied as input. The velocity response resembled the inputs (road profiles), indicating that the response of the wheeled robot can be tracked. Thus, the LQR control system tested was appropriate for controlling a wheeled mobile robot in the agricultural sector.

5. Conclusions

Mathematicians have designed mobile robots with four wheels, but unfortunately using nonholonomic mathematical models for which control or influence is impossible, as confirmed in this study using the concepts of controllable and observables. Based on the expected mathematical models, LQR was selected here as an appropriate control design for a wheeled mobile robot for agricultural use. The primary goal in control is to obtain the best mathematical formula for calculating the Q and R weighting matrices, to overcome the drawbacks of the existing subjective, trial-and-error approaches. Thus, the process seeks to create a strong control framework. The method applied in this study involved computing the matrix Q straight from the state matrix dynamics, here referred to as designer target states. In the situation considered, some states (e.g., altitude and yaw angle) were deemed more essential than the other states, and so the relevant Q values were kept as large as possible to penalize the other states. This Q value was then used to calculate the value of matrix R. The strength of the method lies is its ability to follow changes in the model dynamics caused by defects, uncertainties, and parameter alterations by adjusting the values of the weighting matrix. To assess the performance of the LQR control system, three scenarios were examined (control cheap, non-zero state expensive; control expensive, non-zero state cheap; only non-zero state expensive), with the only costly option being non-zero velocity. Peak time, settling time, rising time, and steady state time for cheap control was determined to be 0.0707 s, 5.53 s, 3.11 s, and 0.0707 s, respectively, based on these scenarios. This indicates that the LQR control system can be appropriate for controlling wheeled mobile robot systems in agricultural applications.

CRediT authorship contribution statement

Sairoel Amertet: Writing – original draft, Writing – review & editing, Validation, Investigation, Funding acquisition, Formal analysis, Data curation, Conceptualization. **Girma Gebresenbet:** Writing – review & editing, Writing – original draft, Supervision, Funding acquisition. **Hassan Mohammed Alwan:** Supervision, Visualization, Writing – review & editing, Writing – original draft.

Declaration of competing interest

There is no conflict of interest.

Data availability

The data that has been used is confidential.

References

[1] G. Adamides, C. Katsanos, G. Christou, M. Xenos, G. Papadavid, T. Hadzilacos, User interface considerations for telerobotics: the case of an agricultural robot sprayer, in: in Second international conference on remote sensing and geoinformation of the environment (RSCy2014), SPIE, 2014, pp. 541–548. Accessed: Oct. 18, 2023. [Online]. Available, https://www.spiedigitallibrary.org/conference-proceedings-of-spie/9229/92291W/User-interface-considerations-for-telerobotics-the-case-of-an/10.1117/12.2068318.short.

[2] K. Ahir, K. Govani, R. Gajera, M. Shah, Application on virtual reality for enhanced education learning, military training and sports, Augment. Hum. Res. 5 (1) (Dec. 2020) 7, https://doi.org/10.1007/s41133-019-0025-2.

[3] F.J. Ostos-Garrido, A.I. De Castro, J. Torres-Sánchez, F. Pistón, J.M. Peña, High-throughput phenotyping of bioethanol potential in cereals using UAV-based multi-spectral imagery, Front. Plant Sci. 10 (2019) 948.

[4] A.S. Elkhatem, S.N. Engin, Robust LQR and LQR-PI control strategies based on adaptive weighting matrix selection for a UAV position and attitude tracking control, Alex. Eng. J. 61 (8) (2022) 6275–6292.

[5] E.C. Suiçmez, Trajectory tracking of a quadrotor unmanned aerial vehicle (uav) via attitude and position control, Master's Thesis, Middle East Technical University, 2014.

[6] J.J. Xiong, E.H. Zheng, Position and attitude tracking control for a quadrotor UAV, ISA Trans 53 (3) (2014) 725–731.

[7] A.A. Najm, I.K. Ibraheem, Altitude and attitude stabilization of UAV quadrotor system using improved active disturbance rejection control," *Arab*, J. Sci. Eng. 45 (3) (Mar. 2020) 1985–1999, https://doi.org/10.1007/s13369-020-04355-3.

[8] N. Koksal, M. Jalalmaab, B. Fidan, Adaptive linear quadratic attitude tracking control of a quadrotor UAV based on IMU sensor data fusion, Sensors 19 (1) (2018) 46.

[9] C. Sun, M. Liu, C. Liu, X. Feng, H. Wu, An industrial quadrotor uav control method based on fuzzy adaptive linear active disturbance rejection control, Electronics (Basel) 10 (4) (2021) 376.
[10] Z. Wang, T. Zhao, Based on robust sliding mode and linear active disturbance rejection control for attitude of quadrotor load UAV, Nonlinear Dyn 108 (4) (Jun. 2022) 3485–3503, https://doi.org/10.1007/s11071-022-07349-y.
[11] E.C. Suicmez, A.T. Kutay, Optimal path tracking control of a quadrotor UAV, in: 2014 International Conference on Unmanned Aircraft Systems (ICUAS), IEEE, 2014, pp. 115–125. Accessed: Oct. 18, 2023. [Online]. Available, https://ieeexplore.ieee.org/abstract/document/6842246/.
[12] L. Li, L. Sun, J. Jin, Survey of advances in control algorithms of quadrotor unmanned aerial vehicle, in: 2015 IEEE 16th international conference on communication technology (ICCT), IEEE, 2015, pp. 107–111. Accessed: Oct. 18, 2023. [Online]. Available, https://ieeexplore.ieee.org/abstract/document/7399803/.
[13] Y. Li, C. Chen, W. Chen, Research on longitudinal control algorithm for flying wing UAV based on LQR technology, Int. J. Smart Sens. Intell. Syst. 6 (5) (Jan. 2013) 2155–2181, https://doi.org/10.21307/ijssis-2017-632.
[14] G. Godinez-Garrido, O.J. Santos-Sánchez, H. Romero-Trejo, O. García-Pérez, Discrete integral optimal controller for quadrotor attitude stabilization: experimental results, Appl. Sci. 13 (16) (2023) 9293.
[15] X. Wei, D. Ye, Z. Zhang, S. Hu, A review of quadrotor control methods, Adv. Eng. Technol. Res. 7 (1) (2023) 495–595.
[16] T. Zhao, W. Li, LQR-based attitude controllers design for a 3-DOF helicopter system with comparative experimental tests, Int. J. Dyn. Control (Jul. 2023), https://doi.org/10.1007/s40435-023-01242-1.
[17] S.J. Chacko, R.J. Abraham, On LQR controller design for an inverted pendulum stabilization, Int. J. Dyn. Control 11 (4) (Aug. 2023) 1584–1592, https://doi.org/10.1007/s40435-022-01079-0.
[18] Z. Qiao, G. Zhu, T. Zhao, Quadrotor cascade control system design based on linear active disturbance rejection control, Appl. Sci. 13 (12) (2023) 6904.
[19] C. Xu, H. Xu, Z. Yang, J. Wu, L. Liao, Q. Zhang, Alternating-direction-method-of-multipliers-based fast model predictive control for an aerial trees-pruning robot, J. Comb. Optim. 46 (1) (Aug. 2023) 6, https://doi.org/10.1007/s10878-023-01071-0.
[20] M. Wang, K. Wang, Q. Zhao, X. Zheng, H. Gao, J. Yu, LQR control and optimization for trajectory tracking of biomimetic robotic fish based on unreal engine, Biomimetics 8 (2) (2023) 236.
[21] C. Liu, Y. Mao, and X. Qiu, "Disturbance-observer-based LQR tracking control for electro-optical system," *In Photonics*, MDPI, 2023, p. 900. Accessed: Oct. 18, 2023. [Online]. Available: https://www.mdpi.com/2304-6732/10/8/900.
[22] S.A. Kouritem, M. Mahmoud, N. Nahas, M.I. Abouheaf, A.M. Saleh, A self-adjusting multi-objective control approach for quadrotors, Alex. Eng. J. 76 (2023) 543–556.
[23] L. Cheng, Y. Li, J. Yuan, J. Ai, Y. Dong, L 1 adaptive control based on dynamic inversion for morphing aircraft, Aerospace 10 (9) (2023) 786.
[24] A.K. Rai, N. Kumar, D. Katiyar, O. Singh, G. Sreekumar, P. Verma, Unlocking productivity potential: the promising role of agricultural robots in enhancing farming efficiency, Int. J. Plant Soil Sci. 35 (18) (2023) 624–633.
[25] J.P. Vásconez, et al., Comparison of path planning methods for robot navigation in simulated agricultural environments, Procedia Comput. Sci. 220 (2023) 898–903.
[26] Y. Bai, B. Zhang, N. Xu, J. Zhou, J. Shi, Z. Diao, Vision-based navigation and guidance for agricultural autonomous vehicles and robots: a review, Comput. Electron. Agric. 205 (2023) 107584.
[27] P. Dziekanski, J. Kochanowski, Smart energy for a smart village: implementation challenges, risks and policies, In Ştiinţă, educaţie, cultură (2023) 452–455. Accessed: Oct. 18, 2023. [Online]. Available, https://ibn.idsi.md/vizualizare_articol/179336.
[28] I.A. Ibrahim, J.M. Truby, FarmTech: regulating the use of digital technologies in the agricultural sector, Food Energy Secur 12 (4) (Jul. 2023) e483, https://doi.org/10.1002/fes3.483.
[29] Y. Wang, J. Fan, S. Yu, S. Cai, X. Guo, C. Zhao, Research advance in phenotype detection robots for agriculture and forestry, Int. J. Agric. Biol. Eng. 16 (1) (2023) 14–25.
[30] M. Ryan, G. Isakhanyan, B. Tekinerdogan, An interdisciplinary approach to artificial intelligence in agriculture, NJAS Impact Agric. Life Sci. 95 (1) (Dec. 2023) 2168568, https://doi.org/10.1080/27685241.2023.2168568.
[31] A.O. Zhukov, A.K. Kulikov, I.N. Kartsan, Optimization of the control algorithm for heterogeneous robotic agricultural monitoring tools, in: IOP Conference Series: Earth and Environmental Science 839, IOP Publishing, 2021 032039.
[32] Shu Li, Liang Ding, Haibo Gao, Yan-Jun Liu, Nan Li, Zongquan Deng, Reinforcement learning neural network-based adaptive control for state and input time-delayed wheeled mobile robots, Systems 50 (11) (2018) 4171–4182.
[33] Arturo. Rojas-Moreno, Predictive LQR control of MIMO time-delay processes possessing output disturbances, in: 2020 IEEE XXVII International Conference on Electronics, Electrical Engineering and Computing (INTERCON), IEEE, 2020, pp. 1–4.
[34] Wouter. Caarls, Deep reinforcement learning with embedded LQR controllers, IFAC-PapersOnLine 53 (2) (2020) 8063–8069.
[35] On Park, Hyosang Shin, Antonios Tsourdos, Linear quadratic tracker with integrator using integral reinforcement learning. In 2019 Workshop On Research, Education and Development of Unmanned Aerial Systems (RED UAS), IEEE, 2019, pp. 31–36.
[36] Sairoel Amertet Finecomes, Fisseha L. Gebre, Abush M. Mesene, Solomon Abebaw, Optimization of automobile active suspension system using minimal order, Internat. J. Elect. Comp. Eng.(IJECE) 12 (3) (2022) 2378–2392.

Sairoel Amertet Finecomes He was born August 30, 1993 in Mizan Aman, South west region of Ethiopia. Attended his primary school at Mizan 2 school and elementary schools at Mizan 1, and Arbaminch. He was attended his high school at Mizan high school and Addis Ababa Dej Azmachi, bright future schools. He received a BSc. degree in Electromechanical Engineering from Hawassa University, Institute of Technology, Hawassa, Ethiopia in 2016, MSc. degree in Mechatronics Engineering from Addis Ababa Science and Technology University, Addis Ababa, Ethiopia, in 2019. He was Lecturer at Mizan Tepi University, Tepi, Ethiopia, and currently he is PHD candidate students at peter the great saint Peterburg university, Russia. His-professional activities have been focused in Software developing, emerging technology, Robotic, Autonomous Technology, hyper automation system, automation agriculture system, Mechatronic systems design, Instrumentation and control, automation of energy, and renewable energy. Currently he is also reviewers for journal IOP. He can be contacted at email: sairoelamertet23@gmail.com.
https://orcid.org/0000-0002-8187-0221
ResearcherID: AGO-5453-2022

Girma Gebresenbet is a Professor, PhD and Head of Division of Automation and Logistics at the Swedish University of Agricultural Sciences, Department of Energy and Technology. His-MSc degree is in Mechanical Engineering and obtained honour degree, specialized in Design and Development. His-PhD is in Agricultural Engineering, and obtained a special reward from the Swedish Academy of Forestry and Agriculture for the outstanding doctoral dissertation of the year. He is a Professor since 2000 and working on Logistics, Transport, and Supply Chain Management. Currently, Gebresenbet is coordinating and managing many national and international research projects, where researchers and industry partners participated from many countries, mainly in the subject areas of Automation in Food Production and Supply chains. He also focuses on Logistics and Supply Chain Management with specific emphasis on City Logistics, Food Supply, Value and Marketing Chain Management in relation to quality, safety (including animal welfare), security, and environment.

Hassan Mohammed Alwan He was born in1962 in Iraq. He received a BSc. degree in Bahgdad university in mechanical Engineering department in Iraq 1984. He was graduated MSc, and PHD from peter the great saint Peterburg polytechnic university, Russia, in 1999, and 2003 respectively. Currently he is a professors at department of mechanical engineering university of technology, Bahgdad, Iraq. His current research interest is robotic and dynamics analysis, theory of machines, robotic systems, control and robotics manipulators.